
1 **Characterization of significant molecular determinants of virulence of** 2 **Enterovirus 71 sub-genotype B4 in Rhabdomyosarcoma cells**

3 **Pinn Tsin Isabel Yee^a, Reham Ahmed Hashim Mohamed^b, Seng-Kai Ong^b, Kuan**
4 **Onn Tan^b, Chit Laa Poh^{a,*}**

5 ^a Research Centre for Biomedical Sciences, School of Science and Technology, Sunway
6 University, Kuala Lumpur, Selangor 47500, Malaysia; isabely@sunway.edu.my.

7 ^b School of Science and Technology, Department of Biological Sciences, School of
8 Science and Technology, Sunway University, Kuala Lumpur, Selangor 47500,
9 Malaysia.

10
11 ***Corresponding Author:** Chit Laa Poh, Sunway University; pohcl@sunway.edu.my

12 **Emails of authors:** isabely@sunway.edu.my, rihoahmed93@gmail.com;
13 ongsk@sunway.edu.my; jefft@sunway.edu.my.

14 **Abstract**

15 One of the leading causes of the hand, foot and mouth disease (HFMD) is Enterovirus 71
16 (EV-A71), displaying symptoms such as fever and ulcers in children but some strains can
17 produce cardiopulmonary oedema which leads to death. There is no FDA-approved
18 vaccine for prevention of severe HFMD. The molecular determinants of virulence for EV-
19 A71 are unclear. It could be a single or a combination of amino acids that determines
20 virulence in different EV-A71 genotype/sub-genotypes. Several EV-A71 strains bearing
21 single nucleotide (nt) mutations were constructed and the contribution of each mutation to
22 virulence was evaluated. The nt(s) that contributed to significant reduction in virulence *in*
23 *vitro* were selected and each mutation was introduced separately into the genome to
24 construct the multiply mutated EV-A71 strain (MMS) which carried six substitutions of
25 nt(s) at the 5'-NTR (U700C), VP1-145 (E to G), VP1-98E, VP1-244K and G64R in the
26 vaccine seed strain that had a partial deletion within the 5'-NTR region (nt. 475-485) of
27 Δ 11bp. In comparison to the wild type strain, the MMS showed low virulence as it
28 produced very low RNA copy number, plaque count, VP1 and had 10⁵-fold higher
29 TCID₅₀, indicative of a promising LAV candidate that should be further evaluated *in vivo*.

30 **Keywords:** enterovirus 71; hand foot mouth disease; virulence; vaccines; codon
31 deoptimization; mutations.

32 **Abbreviations**

33 EV-A71: Enterovirus 71; PV: Poliovirus; 5'-NTR: 5'- non translated region; aa: amino
34 acid; nt: nucleotide; CPE: cytopathic effects; MOI: multiplicity of infection; RD:
35 Rhabdomyosarcoma; PFU: plaque forming units; TCID₅₀: 50% tissue culture infectious
36 dose; VP1: Viral protein; LAV: live attenuated vaccine; MMS: multiply mutated strain.

37 **1. Introduction**

38 In 2016, there were approximately 2.14 million reported cases of Hand, Foot and
39 Mouth Disease (HFMD), including 204 deaths in China (WHO Western Pacific Region
40 Surveillance Summary 2016). Vaccines against the Hand, Foot and Mouth Disease
41 (HFMD) are highly desirable as HFMD has evolved to become a severe global and life
42 threatening disease, ravaging lives of young children in cyclical epidemics in the Asia
43 Pacific. With rising concern about the virulence of EV-A71, there is an urgent need for a
44 vaccine against EV-A71 to be produced that is endorsed by the United States Food and
45 Drug Administration (FDA). Up to date, several biopharmaceutical companies in China
46 have ended their Phase III Clinical Trials, producing the inactivated vaccine (IV)
47 adjuvanted with alum, against the sub-genotype C4a. Although the efficacy of their IVs
48 was more than 90% against mild HFMD, it only conferred 80% protection against severe
49 HFMD (Chong et al., 2015). The IV induces good humoral immunity but is deficient in the
50 cellular arm of immunity, which is needed for long-term protection. Therefore, there is a
51 need to develop other types of vaccines. The development of live attenuated vaccines
52 (LAVs) is desirable as it is known to induce excellent immunogenicity, can elicit both

53 humoral and cellular immunity and able to confer live-long immunity. A LAV from the
54 BrCr strain (S1-3') prototype strain carrying mutations in the 3'-NTR, 3D^{pol} and 5'-NTR
55 was constructed by Arita et al. (2007). Although there was reduced virulence, mild
56 neurological symptoms were still observed in the 3 cynomolgus monkeys immunized with
57 the EV-A71 (S1-3') strain. Hence, the plan to use this strain as a LAV was discontinued
58 (Arita et al., 2007).

59 Before an effective LAV can be developed, there is a need to identify the genetic
60 determinants of virulence. Once the specific determinants of virulence in EV-A71 have
61 been identified, rational design of the LAV can be carried out by site directed mutagenesis
62 (SDM) to target the specific amino acids that are associated with virulence. Classification
63 of genetic determinants of virulence in EV-A71 by analyzing differences in the genome has
64 been published. Sequence comparison between virulent and non-virulent strains showed
65 that 4 amino acids (aa) in VP1 (Gly^{P710}/Gln^{P710}/Arg^{P710}/Glu^{P729}), 1 aa. in the 2A protein
66 (Lys^{P930}) and 4 nucleotides (nt) in the 5'-NTR (G^{P272}, U^{P488} and A^{P700}/U^{P700}) could be
67 genetic determinants for virulent EV-A71 sub-genotype C4 strains (Li et al., 2011). In
68 addition, it was postulated that the EV-A71 mutant displaying high-fidelity (sub-genotype
69 B4) with a single aa. change, (G64R) in its RNA-dependent RNA polymerase (RdRP)
70 enzyme greatly reduced viral pathogenicity *in vivo* (Meng and Kwang, 2014). Kataoka et
71 al. (2015) found that if the aa. glutamic acid was present at position 145 of VP1 (VP1-
72 145E) in EV-A71 (sub-genotype C1), the virus induced neuro-pathogenesis and viremia
73 more efficiently in cynomolgus monkeys than if glycine (G) was found at residue 145
74 (VP1-145G) (Kataoka et al., 2015).

75 The analysis of significant molecular determinants of virulence that were responsible
76 for the attenuated phenotypes of the Sabin Oral Polio Vaccine (OPV) strains was due to the
77 complete sequences of 3 poliovirus (PV) genomes and the development of infectious PV
78 cDNA clones. For example, the Sabin 1 strain differed from its wild type strain with 57 nt.
79 substitutions (Nomoto et al., 1982). It was found that the A480G in the IRES region is the
80 most vital determinant of virulence that contributed to the attenuation in the Sabin 1 strain.
81 It could be possible that nt. 480 affects the formation of a structure in the 5'-NTR
82 responsible for neuro-virulence (Kawamura et al., 1989). For the Sabin 2 strain there were
83 only 2 nt. substitutions (nt. 481 in IRES and nt. 2909 in VP1), whereas a total of 10 nt.
84 substitutions were discovered for the Sabin 3 strain. Amongst the 10, there were 3
85 significant molecular determinants of virulence (C274U in IRES, C2034U in VP3, and
86 U2493C in VP1 (Chia et al., 2014; Huang et al., 2013; Westrop et al., 1989). Virulent
87 strains of EV-A71 are referred to as the new polio as it is neurotropic. Both the
88 enteroviruses share very high sequence homology, particularly in the 5'-NTR. EV-A71
89 contains a similar nt. G481 that is a significant molecular determinant of neuro-virulence in
90 the PV wild type. Hence, studies on PV in earlier research could be good references to
91 design attenuated EV-A71 viruses.

92 With advances in molecular biology, novel approaches to viral attenuation can be
93 further studied such as altered replication fidelity and codon de-optimization. As high
94 mutation rates often hinder the effectiveness of a LAV, increasing the replication fidelity
95 can potentially attenuate whole virus population, culminating to a population collapse with
96 the absence of mutating vital immunogenic epitopes. For all species, codon pair usage is
97 biased and some codon pairs are utilized more often than others (Gutman and Hatfield,
98 1989). A big part of the genetic code is redundant as contiguous pairs of aa. can be coded

99 for by 36 alternate pairs of synonymous codons (Buchan et al., 2006; Sharp et al., 1986).
100 Through the substitution of alternate but synonymous codons within the genome sequence,
101 this would produce different codon pairs but expressing a similar sequence of amino acids.
102 The proteins expressed from these viruses would elicit the same immune response as the
103 wild type viruses. Burns et al. (2006) replaced half of the total codons in the Sabin type 2
104 OPV strain (within capsid region) with less frequently utilized synonymous codons. They
105 discovered that processing and manufacturing of viral proteins were unaffected but viral
106 fitness was reduced (Burns et al., 2006). Subsequently, they replaced natural capsid region
107 codons with synonymous codons that had an abundance of CpG and UpA dinucleotides.
108 Codon-deoptimized PVs were produced and these viruses had significantly lower overall
109 fitness as indicated by lower viral plaque number and virus yields (Burns et al., 2009).

110 Mueller et al. (2006) introduced the biggest number of less frequently utilized
111 synonymous codons in the capsid region of PV type 1 Mahoney. They found a significant
112 decrease in replicative fitness and number of infectious viral progeny. As compared to the
113 wild type, there was also reduction in the viral infectivity up to approximately 1,000-fold
114 and decrease in genome translation (Mueller et al., 2006). The codon deoptimized viruses
115 remained attenuated after repeated cell passages and were genetically stable with minimal
116 risk of reversion (Burns et al., 2006; Mueller et al., 2006). As these viruses have sequences
117 that are fairly divergent from circulating wild type viruses, probabilities for further
118 recombination and production of vaccine-derived variants will be reduced. In addition, the
119 codon deoptimized attenuated viruses were genetically stable and showed low risk of
120 reversion.

121 Previously, we had mutated the EV-A71 virus (sub-genotype B4 virus;
122 5865/Sin/000009) by substitutions at positions 475, 486, and 487 as these 3 nucleotides
123 corresponded to the significant molecular determinants of neuro-virulence in PV Sabin
124 strains 1, 2 and 3. In EV-A71, we have introduced a partial deletion (PD) (deletion from nt.
125 475-485 in the 5'-NTR) as it is considered to be genetically more stable than single site
126 mutations. Compared to mutants with specific nt replacements at 475, 486 and 487, the EV-
127 A71 PD mutant carrying the 11 base pair deletion demonstrated the lowest viral RNA copy
128 number, plaque count and VP1 capsid protein. The PD mutant demonstrated low virulence
129 and therefore, could possibly be a good potential seed strain for designing a LAV candidate
130 (Yee et al., 2016).

131 In this study, we constructed several codon deoptimized EV-A71 viruses by
132 substituting single synonymous codon at positions VP1 (98E), VP1 (242K), VP1 (244K),
133 VP2 (149K) and 2A (930K) to assess the outcome of each codon deoptimization on
134 replication fitness in Rhabdomyosarcoma (RD) cells. If the LAV has single site mutations,
135 there is a strong possibility for reversion to occur. However, if it bears a short deletion and
136 further mutations added to the genome, there is a possibility to reduce reversion and
137 increase the stability of LAVs. In addition, a better attenuated mutant was constructed by
138 introducing multiple mutations into the EV-A71 mutant PD. Hence, we also constructed a
139 multiply mutated EV-A71 strain (MMS) by substituting 6 nucleotides at the 5'-NTR
140 (U700C), VP1-145 (E to G), VP1 (98E), VP1 (242K), VP1 (244K), G64R in the mutant PD
141 (Δ 11bp in 5'-NTR). We evaluated the attenuation of virulence of the MMS in RD cells
142 such as cytopathic effects, viral infectivity by tissue culture infectious dose (TCID₅₀),
143 plaque counts, production of VP1 and RNA copy number.

144 2. Materials and Methods

145 2.1 Tissue culture of RD cell line

146 Human Rhabdomyosarcoma cells (RD, ATCC # CCL-136) were propagated in Dulbecco's
147 modified Eagle's Minimal Medium/F-12 (DMEM/F-12, Invitrogen, USA), that was
148 supplemented with 1.5% NaHCO₃, 10% fetal bovine serum (FBS) (Gibco, USA), 1% non-
149 essential amino acids and 1% penicillin/streptomycin antibiotics. The cells were grown at
150 37°C in 5% CO₂ until they reached confluence.

151 2.2 Virus propagation and storage

152 A 75cm² tissue culture flask with 100% confluent Rhabdomyosarcoma (RD) cells was
153 infected with 100 µl of virus supernatant. The flask was incubated for 1 h at 37°C and
154 replaced with fresh DMEM supplemented with 2% FBS. The flask was incubated at 37°C
155 for 24 - 48h and observed for cytopathic effects (CPE). The culture supernatants were
156 harvested and freeze-thawed 3 times. The supernatants were then centrifuged at 10,000 x g
157 for 20 minutes at 4°C to remove cell debris. The harvested supernatants were then stored at
158 -80°C until further use.

159 2.3 Viral RNA Extraction

160 This process was performed using QIAamp® Viral RNA Mini Kit (Qiagen, Calif., USA).
161 The principle was based on the selective binding properties of a silica-gel based membrane
162 together with micro spin technology to extract viral RNA. The samples were lysed with a
163 buffer which aids in denaturing RNases. The RNA was attached to the membrane which
164 was then washed two times with buffers. The RNA was eluted with DEPC-treated water.

165 An aliquot of 140 µl taken from the samples were processed and the viral RNA was eluted
166 in 50 µl of elution buffer (Qiagen, Calif., USA).

167 *2.4 Reverse transcription of EV-A71 RNA*

168 The purified EV-A71 genomic RNA was converted into cDNA with the SuperScript® IV
169 First Strand Synthesis System (ThermoFisher Scientific, Calif., USA). Each mixture
170 contained 50 mM Tris-HCl (pH 8.3), 4 mM MgCl₂, 10 mM DTT, 50 mM KCl, 0.5 mM
171 dTTP, 0.4 MBq/mL [³H]-dTTP, 0.4 mM poly(A) oligo (dT)₁₂₋₁₈ and SuperScript® IV RT
172 enzyme in 20 µL for 10 min at 37°C.

173 *2.5 Cloning of EV-A71 cDNA into the pCR-XL-TOPO vector*

174 The pCR-XL-TOPO vector was supplied with 3' thymidine (T) overhangs. The PCR
175 products carrying 3' deoxyadenosine (A) overhangs were cloned in the pCR-XL-TOPO
176 vector (Invitrogen, Calif., USA) based on the manual from the manufacturer. About 100
177 ng/µl of the cDNA template was prepared. An aliquot of 4 µl of the cDNA template in TE
178 buffer was mixed with 1 µl (10 ng/µl) of plasmid DNA and incubated at room temperature
179 for 30 min. Thereafter, 1 µl 6X TOPO stop solution was added to prevent the reaction from
180 proceeding further. The recombinant pCR-XL-TOPO_EV71 plasmid was then transformed
181 into *E. coli* XL10-Gold® Ultra competent Cells (Invitrogen, Calif., USA).

182 *2.6 Site-directed mutagenesis*

183 Mutations were introduced by using the QuickChange Lightning Site-Directed Mutagenesis
184 Kit (Agilent Technologies, Calif., USA). A pair of primers consisting the desired mutation
185 was designed for the recombinant pCR-XL-TOPO_EV71 vector. The cycling parameters

186 for the QuikChange Lightning Site-Directed Mutagenesis Method were: 95°C for 2 min for
187 initial denaturation, followed by 18 cycles of 95°C for 20 secs, 60°C for 10 secs, 68°C for 5
188 min 30 sec and 68°C for 5 min for final elongation. Approximately 2 µl of *DpnI* enzyme
189 was added to each amplification reaction to digest the non-mutated supercoiled dsDNA.
190 The enzyme mix was transformed into XL10-Gold ultracompetent *E. coli* cells. Colonies
191 were selected on LB + Kanamycin plate before 3 purified colonies were screened by
192 sequencing.

193 *2.7 Construction of a partial-deletion in the 5'-NTR of EV-A71*

194 A partial deletion (PD) (deletion from nt. 475-485 in the 5'-NTR) was constructed in the
195 EV-A71 genome with a pair of 24-mer forward and 24-mer reverse primers. The mutation
196 was introduced using the Q5® Site-Directed Mutagenesis Kit (New England Biolabs, USA)
197 [(Chua et al., 2008)]. The presence of the deletion was confirmed using the nucleotide
198 Basic Local Alignment Software (BLAST by NCIB).

199 *2.8 Restriction digestion of plasmid DNA*

200 Digestion of pCR-XL-TOPO_EV71 plasmid was carried out with restriction enzyme *EagI*
201 (New England BioLabs, Massachusetts, USA). Briefly, this was carried out in an
202 Eppendorf tube containing 15 µg of plasmid DNA, *EagI* in the corresponding 1X digestion
203 buffer. All reactions were incubated for at least 2 hours at 37°C specified by the
204 manufacturer.

205 *2.9 Phenol-chloroform DNA purification*

206 The linearized DNA was added with an equal volume of phenol/chloroform/isoamyl
207 alcohol (Invitrogen, Calif., USA) and subsequently, vortexed for 1 minute. Solvent and
208 aqueous phases were visible after centrifugation at 15, 000 x g for 10 minutes. The aqueous
209 phase was aspirated and added with an equal volume of chloroform/isoamyl alcohol
210 (Invitrogen, Calif., USA). This step was necessary to remove the remaining phenol. After
211 10 minutes of centrifugation at 15,000 x g, the aqueous phase was aspirated and 1/10
212 volume of 3 M sodium acetate (pH 5.2) was added and vortexed. An aliquot of 1 volume
213 of isopropyl alcohol was added and kept at -20°C for 2 h. The precipitated DNA was
214 centrifuged at 15,000 x g for 30 minutes at 4°C and the DNA pellet was rinsed with 70%
215 ethanol. After air-drying, the pellet was dissolved with TE buffer and DNA concentration
216 determined.

217 *2.10 In vitro transcription of SP6 promoter*

218 RNA transcription was performed utilizing the RiboMAX™ Large Scale RNA Production
219 System-SP6 (Promega, Calif., USA). The reaction mixture was prepared in a 100 µl
220 reaction volume according to the manufacturer's instructions. The reaction mixture was
221 incubated at 37°C for 2 h, followed by addition of DNase for 30 minutes to remove parental
222 DNA. The transcribed RNA was purified with the Illustra Microspin G-50 column (GE
223 Healthcare Life Sciences, Chicago, USA) before transfection in RD cells (Han et al., 2010).

224 *2.11 Transfection of infectious RNA*

225 Overnight grown RD cells (1.5×10^5 cells/well in a 24-well plate) were prepared and used
226 for transfection. Approximately 1µg of RNA was transfected into a well within the 24-well
227 plate. Prior to transfection, the growth medium was removed and replaced with Opti-MEM

228 (Invitrogen, Calif., USA). Transfection mix was prepared with a ratio of 2 μ l of
229 Lipofectamine 2000 reagent to 1 μ g of RNA. The RNA-containing Opti-MEM was mixed
230 with the Lipofectamine 2000 reagent containing Opti-MEM and incubated for 20 min at
231 room temperature. Thereafter, the RNA-lipofectamine mixture was added to the RD cells
232 drop-by-drop. Four hours after transfection, the transfection medium was removed and
233 substituted with 500 μ L 10% FBS DMEM without Penicillin/Streptomycin.

234 *2.12 Quantitation of viral infectivity by tissue culture infectious dose (TCID₅₀) assay*

235 RD cells (3.0×10^4 cells/well in a 96-well plate) were prepared a day before. Using DMEM
236 serum-free media as a diluent, 10-fold serial dilutions of the harvested virus supernatant
237 were carried out in quadruplicates in a 96-well plate. The negative control wells contained
238 infected RD cells (without any virus supernatant). The plate was incubated at 37°C and
239 observed daily for CPE for up to 48h.

240 *2.13 Viral RNA copy determination by real-time RT-PCR*

241 With the RNeasy extraction kit (Qiagen, Calif, USA), viral RNA was extracted from the
242 virus suspension of transfected RD cells. Real-time PCR was carried out utilising the
243 Touch™ Real-Time PCR Detection System (Bio-Rad, CFX96) and the SensiFAST™
244 Probe No-ROX One-Step Kit (BioLine, California, USA). The 20 μ l reaction mixture
245 contained 4 μ l of RNA template, 10 μ l of 2x SensiFAST Probe No-ROX One Step Mix, 0.8
246 μ L forward and reverse primers (10 μ M), 0.2 μ L probe (10 μ M), 0.2 μ l reverse transcriptase
247 enzyme, and 0.4 μ L RiboSafe RNase inhibitor. The reaction was performed for one cycle at
248 48°C for 10 min, 95°C for 2 min, followed by 40 cycles at 95°C for 5s and 60°C for 20s
249 using 0.2 mL PCR tubes and caps (Bio-Rad, Calif, USA).

250 *2.14 VPI determination by western blot*

251 Cellular proteins were extracted from harvested viral suspension of infected cells using
252 RIPA lysis buffer (1.0% Triton X-100, 0.5% sodium deoxycholate, 0.1% sodium dodecyl
253 sulfate, 50 mM Tris, pH 8.0, and protease inhibitor mixture). The protein samples were
254 mixed with an equal volume of 4X SDS protein sample buffer (240 mM Tris-HCl, pH 6.8,
255 8% SDS, 5% β -mercaptoethanol, 40% glycerol and 0.04% bromophenol blue). The protein
256 lysates were run on SDS-PAGE and transferred to nitrocellulose membrane (Millipore,
257 Calif., USA). Thereafter, the membrane was blocked with 5% skim milk powder (Sigma-
258 Aldrich, St Louis, USA) in Tris-Buffered Saline and Tween 20 (TBST) buffer for 1 h on an
259 orbital shaker at room temperature. The membrane was then added with anti-enterovirus
260 VP1 mouse monoclonal primary antibody (Merck, Calif., USA) diluted in 2.5% TBST
261 overnight at 4°C. The next day the nitrocellulose membrane was washed three times with
262 TBST, for 10 min each wash, prior to incubation with anti-mouse HRP secondary antibody
263 (Sigma Aldrich, St Louis, USA) diluted in 2.5% TBST. After hybridization, the membranes
264 were washed three times with TBST, for 10 min each wash, and then detected by chemi-
265 luminescence using ImageQuant (GE Healthcare Life Sciences, Calif., USA).

266 *2.15 Quantitation of viral titer by plaque assay*

267 A 6-well plate with 6×10^5 RD cells/well was seeded before viral infection the subsequent
268 day. Serial 10-fold dilutions of viral suspension were prepared and 1 mL of each dilution
269 was added to the cells for 1 h at 37°C. After viral attachment to the cells, the dilutions were
270 aspirated and substituted with 2 mL of 0.9% w/v high viscosity carboxymethylcellulose
271 (CMC) (Sigma Aldrich, St Louis, USA). After 48 h incubation, the CMC was removed and
272 the cells were fixed with 10% formalin for 10 min. After fixation, the formalin was

273 removed and replaced with 0.5% crystal violet solution for 20 min incubation. The plaques
274 were visible against a white background and the plaque forming units (PFU) were
275 calculated for each EV-A71 mutant.

276 *2.16 Bioinformatics Analysis*

277 The protein sequence of EV-A71 viral proteins was analyzed and the amino acid sequences
278 were aligned with the Clustal method of DNASTAR MegAlign. Predictions of 5'NTR
279 secondary structures of probable base pairs predictions, which might include pseudoknots
280 was conducted by using databases such as RNA Structure at Rochester University:
281 <http://rna.urmc.rochester.edu/RNAstructureWeb/index.html> and the mfold Web Server at
282 http://molbiol-tools.ca/RNA_analysis.htm.

283 *2.17 Statistical Analysis*

284 Based on the data of at least three independent biological replicates, the mean \pm standard
285 deviation was calculated. Statistical significance was determined with the Mann-Whitney
286 test, whereby a p value of < 0.05 was considered as statistically significant.

287 **3. Results**

288 *3.1.1 Cytopathic effects (CPE) caused by EV-A71 mutants*

289 The EV-A71 sub-genotype B4 virus (5865/Sin/000009) was genetically engineered to
290 produce several codon deoptimised EV-A71 viruses by substituting single synonymous
291 codon at positions VP1-98E, VP1-242K, VP1-244K, VP2-149K and 2A-930K. We also
292 substituted several nucleotides (nt) at three positions within the 5'-NTR (C272U, U488C,
293 U700C), VP1-E145G and the 3D^{pol} region (G64R). The effects of these changes were

294 assessed by the inhibition of CPE in RD cells (Table 1). Upon transfection into RD cells
295 with a multiplicity of infection (MOI) of 0.1, mutant C475U still caused the lowest CPE
296 (Figure 1m) when compared to the wild type EV-A71 (Figure 1q). CPE was observed as
297 round cells that lifted off the surface and there was abundant CPE observed with the EV-
298 A71 wild type strain 41 (Figure 1q).

299 Mutant EV-A71 PD caused much lower CPE (Figure 1e) when compared to mutants
300 C272U (Figure 1i) and 2A-930K (Figure 1h). Out of all the mutants, VP2-149K displayed
301 abundant CPE (Figure 1g) as observed from the shrunken and rounding up of many RD
302 cells. Mutants VP1-242K (Figure 1b), U488C (Figure 1j) and A486G (Figure 1n)
303 demonstrated an intermediate amount of CPE after RD cell transfection. Based on the
304 morphology shown in Figure 1c, 1f and 1o, infection of RD cells by mutants VP1-244K,
305 VP1-E145G and G487A showed minimal CPE as cells had the healthy spindle-like shape
306 of multiplying RD cells when compared to EV-A71 wild type sub-genotype B4 (Figure
307 1q). There were not many dead cells floating and showed similar morphology as the negative
308 control (uninfected RD cells) (Figure 1p).

309 A multiply mutated EV-A71 strain (MMS) was constructed by substituting six
310 nucleotides at the 5'-NTR (U700C), VP1-145 (E to G), VP1 (242K), VP1 (98E), VP1
311 (244K), G64R in the strain that consisted of a partial deletion in the 5'-NTR (Δ 11bp). The
312 MMS showed an absence of CPE (Figure 1l), displaying similar morphology as the
313 negative control (Figure 1p). Lower CPE was observed in the MMS in comparison to the
314 codon deoptimised mutant VP1-98E (Figure 1a) and G64R (3D^{pol}) (Figure 1d). The
315 morphology displayed by these EV-A71 mutants showed vast disparity from the abundant
316 CPE observed for the positive control (wild type strain 41) (Figure 1q).

317 3.1.2. Quantitation of viral infectivity by tissue culture infectious dose (TCID₅₀) assay

318 The tissue culture infectious dose (TCID₅₀) is a measurement of the amount of virus
319 that elicits cytopathic effect in 50% of the transfected cell cultures. The MMS demonstrated
320 the highest TCID₅₀ of 3.16×10^8 in comparison to the wild type EV-A71 strain ($2.13 \times$
321 10^3) (Figure 2). This indicates that the MMS would need a significantly higher amount of
322 virus (10^5 -fold more) to elicit a cytopathic effect in 50% of the of the transfected cultures.

323 EV-A71 mutants VP1-E145G and VP1-244K also had 10^5 -fold increased TCID₅₀ value
324 (3.16×10^8) in comparison to the positive control, indicative that the mutants showed a
325 reduction in infectivity. EV-A71 mutants with SDM at VP1-242K (7.02×10^5) and G487A
326 (7.50×10^5) demonstrated greater than 10^2 -fold rise in TCID₅₀ value in comparison to the
327 positive control (EV-A71 wild type). EV-A71 mutant VP1-98E (1.16×10^6) and PD
328 displayed 10^3 -fold increases in TCID₅₀ value in comparison to the wild type (2.13×10^3).
329 An examination of the TCID₅₀ values implicates that mutants carrying single mutations in
330 the VP1, for example, E145G and 244K as well as the MMS required the highest quantity
331 of viruses to elicit cytopathic effect in 50% of the transfected cell cultures. The results
332 indicated a high degree of attenuation in the two SDM mutants and the MMS carrying
333 multiple mutations in its genome (Figure 2).

334 3.1.3 Viral RNA copy determination by real-time RT-PCR

335 Assays such as the viral RNA copy number quantitation and TCID₅₀ of various
336 mutant strains will allow a better quantitative comparison of the growth aspects of the

337 different mutant strains. The viral RNA copy number of the EV-A71 mutant strains was
338 assessed after transfection into RD cells. The positive control (wild type strain 41)
339 produced the highest amount of viral RNA copy number (5.8×10^4). Significantly lower
340 RNA copy numbers were detected for mutants C475U (1.02×10^2) and PD (1.05×10^2)
341 (Figure 3). When the mutant strains were examined in RD cells, a few new mutations seem
342 to decrease viral replication. It was demonstrated that mutant VP1-244K gave a yield of 2.9
343 $\times 10^2$ RNA copy number which was 100-times lesser than the positive control viral RNA
344 copy number (5.8×10^4). It appeared that mutant VP2-149K yielded the greatest amount of
345 viral RNA copy number of 2.9×10^4 in comparison to the positive control (wild type strain
346 41). As the RNA copy number is still approximately half to that of the wild type strain, this
347 shows that there remains some degree of attenuation.

348 In addition, the mutant VP1-E145G displayed significant decreases in viral RNA copy
349 number (4.5×10^2) (Figure 3). The MMS yielded markedly low viral RNA copy number of
350 1.3×10^2 and substantially decreased the viral RNA copy number to almost 10²-fold less in
351 comparison to the positive control (5.8×10^4). A reduction of RNA copy number was also
352 expressed by mutants VP1-98E and G64R (3D^{pol}) at 7.8×10^2 and 1.4×10^3 , respectively.

353 *3.1.4 VP1 determination by western blot*

354 Western blotting with monoclonal antibodies targeted at the VP1 capsid protein of
355 EV-A71 could enable the detection of the viral capsid protein and be an indirect indicator
356 of the ability of the various mutant strains to produce viable viral particles. Cellular protein

lysate was harvested from the supernatants of infected RD cells and sodium dodecyl sulfate polyacrylamide gel electrophoresis (SDS-PAGE) was performed to separate the EV-A71 proteins based on molecular weight (MW). A singular band was revealed at a MW of 37 kDa which corresponds to the VP1 monomer (Figure 4).

Based on the Western blot analysis, cellular proteins from RD cells transfected with the positive control (wild type EV-A71) (Figure 4, Lane 16) showed the greatest VP1 protein amount (36 kDa). There was hardly any VP1 observed for mutant C475U (Figure 4, Lane 8), mutant G487A (Figure 4, Lane 5) and mutant PD (Figure 4, Lane 13). The results were consistent with the cytopathic effect, TCID₅₀ infectivity and viral RNA copy number. There seems to be a few nt. in the EV-A71 viral genome that are attenuating the virus as the quantity of VP1 for some of the mutant strains were significantly lesser than the positive control (Figure 4, Lane 16). The mutant MMS (Figure 4, Lane 6), mutant VP1-244K (Figure 4, Lane 10) and mutant VP1-E145G (Figure 4, Lane 3) showed much lesser VP1 quantity in comparison to the positive control (wild type strain 41) (Figure 4, Lane 16). Although each mutant had caused significant reduction of virulence in terms of VP1, viral RNA copy number, and TCID₅₀ values, the introduction of all the mutations together in a single genome will enable increased genetic stability.

3.1.5 Quantitation of viral titre by plaque assay

Plaque numbers produced by the different EV-A71 mutants were assessed in RD cells by plaque assays. Our objective is to evaluate the ability of the various mutants to

377 form plaques. RD cells infected with the positive control (wild type EV-A71 strain 41)
378 gave the largest plaque number (8.0×10^8 PFU/mL). The smallest plaque numbers were
379 produced by the MMS (1.2×10^4 PFU/mL) and mutant C475U (7.0×10^4 PFU/mL) (Figure
380 5).

381 Based on Figure 6, there are a few nt. in EV-71 viral genome that appear to attenuate the
382 virus. The EV-A71 mutant VP1-E145G gave a yield of 3.5×10^5 PFU/ml and the mutant
383 VP1-244K produced a decrease in number of plaques (2.5×10^5 PFU/ml) in comparison to
384 the EV-A71 wild type (5865/Sin/000009), although the plaque counts were higher than the
385 mutant PD (1.0×10^5 PFU/mL). The mutant VP1-98E also showed reduced plaque number
386 (7.5×10^5 PFU/mL). As there was reduction in viral growth, this was indicative that the
387 plaque forming capability has been decreased markedly for several mutant strains. This
388 signifies that there would be weaker viremia due to a reduction in viral copy number as
389 viral load induces pathogenicity.

390 **4. Discussion**

391 In our previous investigation, we genetically engineered the EV-A71 sub-genotype B4
392 (5865/Sin/000009) through site directed mutagenesis via the substitution of nt. at positions
393 475, 486, and 487 as these nts. were the molecular determinants of neurovirulence in PV
394 Sabin strains 1, 2 and 3. We also introduced a partial deletant (PD) in the 5'-NTR region
395 (deletion from nt. 475-485 in the 5'-NTR) as it may be genetically more stable than single
396 site mutations. The study concluded that the EV-A71 partial deletant (PD) and mutant 475
397 demonstrated the lowest RNA copy number, plaques and VP1 protein followed by EV-A71

398 mutants 487, 5262, 158 and 486 in the order listed. This shows that the mutant PD could
399 serve as a potential vaccine seed strain to carry beneficial mutations that will further
400 attenuate or stabilize it to become a good LAV candidate (Yee et al., 2016).

401 In addition, better attenuated mutants could be constructed by introducing multiple
402 mutations into the attenuated EV-A71 mutant PD. With advances in molecular biology,
403 novel approaches to viral attenuation can be further studied such as altered replication
404 fidelity and codon deoptimization. As for the latter approach, synonymous codons can be
405 substituted all over a viral genome, hence preventing a decrease in immunogenicity and
406 minimal possibility of reversion to wild type virulence. Studies on codon bias on viral
407 multiplication and pathogenicity of poliovirus (PV) have been reported (Burns et al., 2009;
408 Mueller et al., 2006). Interestingly, many studies have discovered that the deoptimized
409 viruses remained attenuated after repeated passages and hence, were genetically stable with
410 minimal risk of reversion. As both PV and EV-A71 share very high percentage of sequence
411 homology hence, the codon deoptimization research on PV published in recent work could
412 be referred to in the production of highly attenuated EV-A71 viruses. Therefore, we
413 constructed several codon deoptimized EV-A71 viruses by substituting synonymous codon
414 at positions VP1 (98E), VP1 (244K), VP1 (244K), VP2 (149K) and 2A (930K) to evaluate
415 the effect of each codon deoptimization on replication fitness in Rhabdomyosarcoma (RD)
416 cells.

417 Thus far, there is no quantification of the effects of different amino acids in the viral
418 genome on virulence except for studies of comparison of nt. and amino acid sequences
419 between virulent and non-virulent strains. In addition, most of the studies using
420 comparative analysis between the strains were of sub-genotype C4. For example, 4 aa.

421 differences in the VP1 region (Gly^{P710}/Gln^{P710}/Arg^{P710}/Glu^{P729}), Lys^{P930} in 2A region and 4
422 nts. in the 5'-NTR region (A^{P700}/U^{P700}, G^{P272}, U^{P488}) were found after aligning the VP1
423 sequences between fatal and mild EV-A71 strains (sub-genotype C4) (Li et al., 2011).
424 These aa. demonstrate that there were several genetic determinants for virulent EV-A71
425 strains and these aa. could possibly be responsible in changing mild strains into fatal ones.
426 This is to be expected as the 5'-NTR was responsible for cap-independent translation of
427 viral proteins. As such, research reported in the study by Li et al. (2011) served as a
428 reference to assess quantitatively the degree of attenuation of EV-A71 mutants constructed
429 in this study to carry mutations C272U, U488C and U700C in the viral genome.

430 The importance of a C104U nt. substitution in the 5'-NTR region (between the
431 cloverleaf and stem-loop II region) of CV-A16 was first demonstrated by Li et al. (2016).
432 This mutation could significantly lower RNA replication and inhibit translational activity *in*
433 *vitro* and also in the neonatal ICR mice. They identified that the nt. C104U could possibly
434 be a molecular determinant of virulence for the lethal CV-A16 strain. The mutation affected
435 the binding of the heterogeneous nuclear ribonucleoprotein K (hnRNP K) and A1 (hnRNP
436 A1) with the 5'-NTR, hence reducing translational rates. This was discovered by aligning
437 with nt. sequences in the 5'-NTR of the prototype G10, the non-lethal SHZH05 strains and
438 the lethal Changchun024 strain. Thereby, the authors constructed infectious mutants of CV-
439 A16 with different nt. substitutions in the 5'-NTR (Li et al., 2016). Similar to the finding
440 that the 5'-NTR region is also carrying the specific genetic determinants for virulent EV-
441 A71 sub-genotype C4 strains, this study reporting specific nt. changes in the 5'-NTR of
442 CV-A16 with subsequent reductions in viral replication lends credence that the 5'-NTR
443 region is a virulence-associated site.

444 In addition, Caine et al. (2016) discovered that a single mutation in VP1-244 (K244E)
445 was crucial for mouse-adapted EV-A71 (mEV-A71) virulence and expanded tissue tropism
446 in adult interferon-deficient AG129 mice. They also found a new VP1 mutation (H37R)
447 that was important for K244E recovery in primate cell culture (Vero cells). The authors
448 postulated that the H37R/K244E interaction is pertinent for replication in primate cells but
449 the K244E mutant could replicate alone in a murine model (Caine et al., 2016). Three
450 positions were demonstrated to be conserved among neurovirulent strains but were
451 different from sub-genotype C4a strains carrying mild HFMD (Val^{P1148}/Ile^{P1148} in 3A,
452 Val^{P814}/Ile^{P814} in VP1, Ala^{P1728}/Cys^{P1728}/Val^{P1728} in 3C). These amino acid residues may be
453 potential genetic determinants of virulence. Amongst all the 3 neurovirulent strains,
454 SDLY107 varied in 4 nts. (C^{P579}/T^{P579}, C^{P241}/T^{P241}, A^{P571}/T^{P571} in 5'-NTR and T^{P7335}/C^{P7335}
455 in 3'-NTR), suggesting that these nt(s). may be genetic determinants of virulence (Wen et
456 al., 2013). Liu et al. (2014) discovered that there were 9 aa. differences in the VP1
457 sequences (E145G/Q, V249I, H22Q, P27S, N31S/D, E98K, D164E, T240A/S, A289T) in a
458 comparison between fatal and mild EV-A71 strains (sub-genotype C4). These aa. could be
459 possible genetic determinants of virulence in EV-A71 that could convert mild strains into
460 fatal ones (Liu et al., 2014). The position of a single or a combination of aa. may have deep
461 implications for virulence in different EV-A71 genotype/sub-genotype strains.

462 Wang et al. (2012) performed analysis on seven EV-A71 sequences (sub-genotype C4)
463 from HFMD patients in Changchun, China who suffered either mild or severe HFMD.
464 They identified that these seven viruses were actually recombinant viruses evolved from
465 different type A Enteroviruses. For example, these viruses contained genetic recombination
466 events between CV-A4, CV-A5, and EV-A71 (sub-genotypes B4 and C1) and hence not
467 surprisingly, most of the structural protein, P1 of these viruses resembled that of the

468 prototype EV-A71, sub-genotype C1 strains. There was also a very high amount of
469 similarity between the non-structural proteins (P2 and P3) and CV-A4, CV-A5, with EV-
470 A71 (sub-genotype B4) in varying genomic regions possibly due to genomic recombination
471 events. As our viral strain was also of sub-genotype B4, our working strain may have
472 evolved from a single common ancestor that had continuously evolved over the years. This
473 has serious implications as a virus that continuously undergoes genetic recombination could
474 lead to the evolution of more virulent viruses. This would then make designing of a vaccine
475 more difficult for such viruses that have high mutability rates (Wang et al., 2012). Hence,
476 further studies such as phylogenetic analysis of isolates from mild/severe patients infected
477 with EV-A71 (sub-genotype B4) should be carried out to determine the pattern of
478 evolution.

479 Interestingly, when Threonine at position 251 within the 3D^{Pol} region was substituted
480 with Isoleucine (T251I), it altered the temperature susceptibility of EV-A71 (sub-genotype
481 C2) from total susceptibility to complete resistance at 39.5°C *in vitro*. This strain also had
482 increased viral virulence and showed clinical symptoms *in vivo* (Huang et al., 2015). The
483 pathogenicity of mutant T251I was not evaluated in our investigation as the EV-A71 strain
484 41 (sub-genotype B4) does not carry a threonine (T) at residue 251 when compared to the
485 sub-genotype C2 in the study conducted by Huang et al. (2015). However, we constructed a
486 mutant similar to that of Meng and Kwang (2014) who produced highly attenuated EV-A71
487 mutants displaying high-fidelity with a single aa. change, (G64R) in its RdRP that greatly
488 reduced pathogenicity *in vivo*. These EV-A71 mutants have lower pathogenicity as they are
489 unable to generate replication-efficient mutations and have much lower genetic diversity to
490 withstand a wide range of selective pressures. The authors postulate that the G64R mutant

491 could serve as a promising vaccine candidate as G64R mutant was genetically stable in the
492 brain and muscle of infected mice at 12th-day post-infection (Meng and Kwang, 2014).

493 Kataoka et al. (2013) discovered that if glutamic acid (E) was present at aa. VP1-145
494 (sub-genotype C1), the virus induced neuro-pathogenesis and viremia more efficiently in
495 cynomolgus monkeys than if glycine (G) was found at residue 145 (Kataoka et al., 2015). It
496 was also demonstrated that the E145Q substitution within the VP1 region was a frequent
497 change in the EV-A71 viral genomes of strains associated with mild and fatal HFMD cases.
498 Generally, fatal strains had more substitutions in the IRES and 5'-NTR regions (Chang et
499 al., 2012). This was of no surprise as these regions were responsible for receptor binding
500 and translation of viral mRNA. The VP1-145 amino acid has been determined as a “hot
501 spot” for evolutionary pressures on EV-A71 (Tee et al., 2010). In order to investigate the
502 involvement of VP1-145 and G64R in the molecular basis of virulence in EV-A71 sub-
503 genotype B4, site directed mutagenesis at positions G64R and VP1-E145G was conducted
504 at these 2 sites to analyze the effects of both the mutations on virulence.

505 However, one of the disadvantages of a LAV would be its potential to revert back to
506 wild type virulence, especially if the strain consists of “hot spots” for mutations. Hence, to
507 boost the genetic stability of the LAV, multiple mutations were further introduced into the
508 EV-A71 genome to reduce reversion and increase the stability of LAVs. The virulence of
509 the different EV-A71 mutant strains was evaluated in the RD cell line by cytopathic effects,
510 viral titer by tissue culture infectious dose (TCID₅₀), plaque assays, detection of VP1 and
511 real time determination of RNA copy number. After the effects brought about by each of
512 the single site mutation and the partial deletion were quantified, the most significant
513 mutations that could reduce virulence were selected and introduced into the PD mutant.

514 Hence, we had constructed a multiply mutated EV-A71 strain (MMS) by substituting six
515 different nucleotides at U700C, VP1-E145G, VP1-242K, VP1-98E, VP1-244K, G64R
516 (3D^{pol}) in the strain carrying a partial deletant (Δ 11bp) within the 5'-NTR region.

517 Very little VP1 quantity was observed in the EV-A71 mutants having site specific
518 mutations at nt. 475 and 487 in the 5'-NTR. An examination of the TCID₅₀ values showed
519 that the MMS needed significantly greater viral titer (3.16×10^8) to show CPE in 50% of
520 the infected cells. This was to be expected as the MMS had lower infectivity in RD cells
521 than the other codon deoptimized and SDM mutants. Significantly lower RNA copy
522 numbers were obtained for 3 mutants (MMS, VP1-244K, VP1-E145G) at 1.3×10^2 , $2.9 \times$
523 10^2 , and 4.5×10^2 , respectively. Although the MMS could not totally eradicate viral
524 replication, there was significant 10^5 -fold decrease in viral growth.

525 Subsequently, the number of plaques produced by the various mutant strains was
526 examined in RD tissue culture by plaque assays. If the capability to form plaques is
527 reduced, this would mean that viral growth is slower, thereby producing a lower PFU/ml
528 value. For example, the mutant VP1-244K (2.5×10^5 PFU/mL) and mutant VP1-E145G
529 showed significant decreases in plaque count (3.5×10^5 PFU/mL) in comparison to the EV-
530 A71 wild type (strain 41) with 8.0×10^8 PFU/mL. The lowest plaque count was formed by
531 the MMS (1.2×10^4 PFU/mL) and mutant C475U (7.0×10^4 PFU/mL).

532 Some of the site directed mutations such as those introduced into sites at 475, 487,
533 VP1-145, VP1-244 and a deletion in mutant PD were very effective in reducing cytopathic
534 effects, RNA copy numbers, plaque count, VP1 amount and TCID₅₀. By combining the
535 beneficial mutations into a single vaccine strain, the MMS may serve as a potential LAV
536 candidate for further evaluation by virulence testing *in vivo*. Attenuated strains with low

537 viral RNA copy number are possible good vaccine strains as they could not replicate fast
538 enough to yield high viral load and cause destruction of the tissue cells. Slow replication
539 could infer that the cells could still carry enough antigens to stimulate a good immune
540 response.

541 **5. Conclusions**

542 This investigation has isolated and characterized several EV-A71 mutants with
543 significant attenuation of viral virulence in Rhabdomyosarcoma cells. Better attenuated
544 mutants could be constructed by introducing multiple mutations into the attenuated EV-
545 A71 mutant PD. It was discovered that EV-A71 mutants carrying mutations at C272U,
546 U488C and U700C in the 5'-NTR were not highly attenuated as they still produced more
547 RNA, VP1 protein, plaque count and had lower TCID₅₀ values than other SDM and codon
548 deoptimized mutants. Therefore, they are not significant virulence determinants for the wild
549 type EV-A71 strain 41 (sub-genotype B4) in comparison to the sub-genotype C4 fatal
550 strains studied by Li et al. (2011) (Li et al., 2011). The multiple mutations in the MMS did
551 not totally eradicate the capability of the virus to multiply *in vitro*, but there were
552 significant decreases in replication. Further studies should be conducted to investigate the
553 stability of the MMS. A strain which is genetically highly stable and does not revert easily
554 would thereby make a better LAV for EV-A71.

555 The results support the hypothesis that every EV-A71 genotype or sub-genotype carries
556 a different virulence determinant or a combination of significant virulence determinants. In
557 a particular sub-genotype, there may be several amino acids that determine virulence; hence
558 it is important to identify significant amino acid residues that could be combined in the
559 rational design of effective LAVs Therefore, the results obtained in this study demonstrate

560 that quantifying the reduction of virulence through comparison of each SDM and partial
561 deletion introduced into the genome is more effective than comparison of sequences
562 between fatal and non-fatal strains.

563 **Acknowledgments**

564 We are very appreciative of the support of the Fundamental Research Grant Scheme
565 [FRGS/2/2014/ST03/SYUC/1]; Sunway University Internal Grants [INT-RRO-2014-017
566 and INT-VCO-0214-01] and the Sunway University Vice-Chancellor Fellowship to Isabel
567 Yee. The grants funded the research consumables required for the execution of the project.

568 **Author Contributions:** PT Yee and CL Poh conceived and accomplished the project. PT
569 Yee and CL Poh designed the experiments. Tan KO provided molecular biology advice and
570 guidance. PT Yee performed the experiments. Tan KO and Ong SK provided critique to the
571 article. PT Yee analyzed the data and prepared the article. All authors have read and
572 approved the article.

573 **Conflicts of Interest:** All authors declare no conflict of interest.

574 **References**

- 575 Arita, M., Nagata, N., Iwata, N., Ami, Y., Suzaki, Y., Mizuta, K., Iwasaki, T., Sata, T.,
576 Wakita, T., Shimizu, H., 2007. An Attenuated Strain of Enterovirus 71 Belonging to
577 Genotype A Showed a Broad Spectrum of Antigenicity with Attenuated
578 Neurovirulence in Cynomolgus Monkeys. *J. Virol.* 81, 9386–9395.
579 doi:10.1128/JVI.02856-06
- 580 Buchan, J.R., Aucott, L.S., Stansfield, I., 2006. tRNA properties help shape codon pair

- 581 preferences in open reading frames. *Nucleic Acids Res.* 34, 1015–1027.
582 doi:10.1093/nar/gkj488
- 583 Burns, C.C., Campagnoli, R., Shaw, J., Vincent, A., Jorba, J., Kew, O., 2009. Genetic
584 Inactivation of Poliovirus Infectivity by Increasing the Frequencies of CpG and UpA
585 Dinucleotides within and across Synonymous Capsid Region Codons. *J. Virol.* 83,
586 9957–9969. doi:10.1128/JVI.00508-09
- 587 Burns, C.C., Shaw, J., Campagnoli, R., Jorba, J., Vincent, A., Quay, J., Kew, O., 2006.
588 Modulation of Poliovirus Replicative Fitness in HeLa Cells by Deoptimization of
589 Synonymous Codon Usage in the Capsid Region. *J. Virol.* 80, 3259–3272.
590 doi:10.1128/JVI.80.7.3259-3272.2006
- 591 Caine, E.A., Moncla, L.H., Ronderos, M.D., Friedrich, T.C., Osorio, J.E., 2016. A Single
592 Mutation in the VP1 of Enterovirus 71 Is Responsible for Increased Virulence and
593 Neurotropism in Adult Interferon-Deficient Mice. *J. Virol.* 90, 8592–8604.
594 doi:10.1128/JVI.01370-16
- 595 Chang, S.-C., Li, W.-C., Chen, G.-W., Tsao, K.-C., Huang, C.-G., Huang, Y.-C., Chiu, C.-
596 H., Kuo, C.-Y., Tsai, K.-N., Shih, S.-R., Lin, T.-Y., 2012. Genetic characterization of
597 enterovirus 71 isolated from patients with severe disease by comparative analysis of
598 complete genomes. *J. Med. Virol.* 84, 931–939. doi:10.1002/jmv.23287

- 599 Chia, M.Y., Chung, W.Y., Chiang, P.S., Chien, Y.S., Ho, M.S., Lee, M.S., 2014.
600 Monitoring Antigenic Variations of Enterovirus 71: Implications for Virus
601 Surveillance and Vaccine Development. *PLoS Negl. Trop. Dis.* 8.
602 doi:10.1371/journal.pntd.0003044
- 603 Chong, P., Liu, C.C., Chow, Y.H., Chou, A.H., Klein, M., 2015. Review of enterovirus 71
604 vaccines. *Clin. Infect. Dis.* doi:10.1093/cid/ciu852
- 605 Chua, B.H., Phuektes, P., Sanders, S.A., Nicholls, P.K., McMinn, P.C., 2008. The
606 molecular basis of mouse adaptation by human enterovirus 71. *J. Gen. Virol.* 89,
607 1622–1632. doi:10.1099/vir.0.83676-0
- 608 Gutman, G.A., Hatfield, G.W., 1989. Nonrandom utilization of codon pairs in *Escherichia*
609 *coli*. *Proc. Natl. Acad. Sci.* 86, 3699–3703. doi:10.1073/pnas.86.10.3699
- 610 Han, J.-F., Cao, R.-Y., Tian, X., Yu, M., Qin, E.-D., Qin, C.-F., 2010. Producing infectious
611 enterovirus type 71 in a rapid strategy. *Virol. J.* 7, 116. doi:10.1186/1743-422X-7-116
- 612 Huang, M.L., Chiang, P.S., Chia, M.Y., Luo, S.T., Chang, L.Y., Lin, T.Y., Ho, M.S., Lee,
613 M.S., 2013. Cross-reactive neutralizing antibody responses to enterovirus 71
614 infections in young children: implications for vaccine development. *PLoS Negl Trop*
615 *Dis* 7, e2067. doi:10.1371/journal.pntd.0002067
- 616 Huang, S.-W., Tai, C.-H., Fonville, J.M., Lin, C.-H., Wang, S.-M., Liu, C.-C., Su, I.-J.,

- 617 Smith, D.J., Wang, J.-R., 2015. Mapping Enterovirus A71 Antigenic Determinants
618 from Viral Evolution. *J. Virol.* 89, 11500–6. doi:10.1128/JVI.02035-15
- 619 Kataoka, C., Suzuki, T., Kotani, O., Iwata-Yoshikawa, N., Nagata, N., Ami, Y., Wakita, T.,
620 Nishimura, Y., Shimizu, H., 2015. The Role of VP1 Amino Acid Residue 145 of
621 Enterovirus 71 in Viral Fitness and Pathogenesis in a Cynomolgus Monkey Model.
622 *PLoS Pathog.* 11. doi:10.1371/journal.ppat.1005033
- 623 Kawamura, N., Kohara, M., Abe, S., Komatsu, T., Tago, K., Arita, M., Nomoto, A., 1989.
624 Determinants in the 5' noncoding region of poliovirus Sabin 1 RNA that influence the
625 attenuation phenotype. *J. Virol.* 63, 1302–9.
- 626 Li, R., Zou, Q., Chen, L., Zhang, H., Wang, Y., 2011. Molecular analysis of virulent
627 determinants of enterovirus 71. *PLoS One* 6. doi:10.1371/journal.pone.0026237
- 628 Li, Z., Liu, X., Wang, S., Li, J., Hou, M., Liu, G., Zhang, W., Yu, X.-F., 2016.
629 Identification of a nucleotide in 5' untranslated region contributing to virus replication
630 and virulence of Coxsackievirus A16. *Sci. Rep.* 6, 20839. doi:10.1038/srep20839
- 631 Liu, Y., Fu, C., Wu, S., Chen, X., Shi, Y., Zhou, B., Zhang, L., Zhang, F., Wang, Z., Zhang,
632 Y., Fan, C., Han, S., Yin, J., Peng, B., Liu, W., He, X., 2014. A novel finding for
633 enterovirus virulence from the capsid protein VP1 of EV71 circulating in mainland
634 China. *Virus Genes* 48, 260–272. doi:10.1007/s11262-014-1035-2

- 635 Meng, T., Kwang, J., 2014. Attenuation of Human Enterovirus 71 High-Replication-
636 Fidelity Variants in AG129 Mice. *J. Virol.* 88, 5803–5815. doi:10.1128/JVI.00289-14
- 637 Mueller, S., Papamichail, D., Coleman, J.R., Skiena, S., Wimmer, E., 2006. Reduction of
638 the Rate of Poliovirus Protein Synthesis through Large-Scale Codon Deoptimization
639 Causes Attenuation of Viral Virulence by Lowering Specific Infectivity. *J. Virol.* 80,
640 9687–9696. doi:10.1128/JVI.00738-06
- 641 Nomoto, A., Omata, T., Toyoda, H., Kuge, S., Horie, H., Kataoka, Y., Genba, Y., Nakano,
642 Y., Imura, N., 1982. Complete nucleotide sequence of the attenuated poliovirus Sabin
643 1 strain genome. *Proc. Natl. Acad. Sci. U. S. A.* 79, 5793–5797.
644 doi:10.1073/pnas.79.19.5793
- 645 Sharp, P.M., Tuohy, T.M.F., Mosurski, K.R., 1986. Codon usage in yeast: Cluster analysis
646 clearly differentiates highly and lowly expressed genes. *Nucleic Acids Res.* 14, 5125–
647 5143. doi:10.1093/nar/14.13.5125
- 648 Tee, K.K., Lam, T.T.-Y., Chan, Y.F., Bible, J.M., Kamarulzaman, A., Tong, C.Y.W.,
649 Takebe, Y., Pybus, O.G., 2010. Evolutionary Genetics of Human Enterovirus 71:
650 Origin, Population Dynamics, Natural Selection, and Seasonal Periodicity of the VP1
651 Gene. *J. Virol.* 84, 3339–3350. doi:10.1128/JVI.01019-09
- 652 Wang, X., Zhu, C., Bao, W., Zhao, K., Niu, J., Yu, X.-F., Zhang, W., 2012.

- 653 Characterization of Full-Length Enterovirus 71 Strains from Severe and Mild Disease
654 Patients in Northeastern China. PLoS One 7, e32405.
655 doi:10.1371/journal.pone.0032405
- 656 Wen, H.L., Si, L.Y., Yuan, X.J., Hao, S.B., Gao, F., Chu, F.L., Sun, C.X., Wang, Z.Y.,
657 2013. Complete genome sequencing and analysis of six enterovirus 71 strains with
658 different clinical phenotypes. Virol J 10, 115. doi:10.1186/1743-422x-10-115
- 659 Westrop, G.D., Wareham, K.A., Evans, D.M., Dunn, G., Minor, P.D., Magrath, D.I., Taffs,
660 F., Marsden, S., Skinner, M.A., Schild, G.C., 1989. Genetic basis of attenuation of the
661 Sabin type 3 oral poliovirus vaccine. J. Virol. 63, 1338–44.
- 662 World Health Organization, 2016. Hand, foot, and mouth disease situation update number
663 503.http://www.wpro.who.int/emerging_diseases/hfmd_biweekly_20161018.pdf?ua=1
664 (accessed 12.05.17).
- 665 Yee, P.T.I., Tan, K.O., Othman, I., Poh, C.L., 2016. Identification of molecular
666 determinants of cell culture growth characteristics of Enterovirus 71. Virol. J. 13, 194.
667 doi:10.1186/s12985-016-0645-9
668
669

670 **Table 1.** Cytopathic effects (CPE) caused by EV-A71 mutants and the positive control
 671 (wild type EV-A71 sub-genotype B4).

EV-A71 Mutants	CPE
C475U	+
A486G	+++
G487A	+
VP1-98E	++
VP1-242K	+++
VP1-244K	+
G64R (3D ^{pol})	++
Partial Deletant (PD) 5'-NTR	+
VP1-E145G	+
VP2-149K	++++
2A-930K	++++
C272U	+++
U488C	+++
C700U	++
Multiple Mutant strain (MMS)	+
Positive control (wild type EV-A71)	+++++

672 RD cells were infected with EV-A71 mutants and the positive control (wild type EV-A71
 673 sub-genotype B4) at a multiplicity of infection (MOI) of 0.1.

Figure 1. CPE by EV-A71 mutants (a) VP1-98E (b) VP1-242K (c) VP1-244K (d) G64R (e) PD (f) VP1-E145G (g) VP2-149K (h) 930K (2A) (i) C272U (j) U488C (k) C700U (l) Multiple Mutant strain (MMS) (m) C475U (n) A486G (o) G487A in RD cells compared with (p) uninfected RD cells (negative control) and (q) infected RD cells (positive control).

Figure 2. Logarithm Tissue Culture Infectious Dose 50 (Log TCID₅₀) of EV-A71 mutants compared with the positive control (EV-A71 sub-genotype B4). The plate was placed at 37°C for up to 48h and observed daily for CPE. The TCID₅₀/ml values are determined based on the Reed and Muench formula from at least three independent experiments.

Figure 3. Viral RNA copy number quantification. Transfection of infectious RNA of EV-A71 mutants into RD cells was carried out with Lipofectamine 3000 reagent with a MOI of 0.1. (+) control refers to wild type EV-A71 sub-genotype B4. (-) control refers to RD cells with no virus infection. The RNA copy number was calculated at 24h post-infection by TaqMan Real-Time PCR based on the average of at least three biological replicates. Error bars indicate the standard deviation \pm mean.

Figure 4. Western blot using monoclonal antibodies against VP1 as the primary antibody. The quantity of total proteins from EV-A71 and β -actin in each lane was 20 μ g. The lanes are as follows: lane M, molecular weight marker (from 10 - 250 kilodaltons), lane 1, Mutant G64R; lane 2, Mutant VP1-98E; lane 3, Mutant VP1-E145G; lane 4, Mutant U488C; lane 5, Mutant G487A; lane 6, MMS; lane 7, A486G; lane 8, C475U; lane 9, Mutant VP1-242K; lane 10, Mutant VP1-244K; lane 11, Mutant C272U; lane 12, Mutant U700C; lane 13, Mutant Partial Deletant (PD); lane 14, VP2-149K; lane 15, 2A-930K; lane 16, Positive control (EV-A71 strain 41); lane 17, Negative control (non-infected cells). The molecular weights of the VP1 protein and β -actin are 36 kDa and 42 kDa, respectively.

Figure 5. Quantification of plaque counts by EV-A71 mutants and positive control (wild type EV-A71). The plaque assays were carried out on RD cells incubated at 37°C for 48h from at least two independent experiments.

Figure 6. Plaque Forming Units (PFU) by EV-A71 mutants in comparison with the positive control (wild type EV-A71). RD cells were transfected with EV-A71 mutants and the positive control at a MOI of 0.1. Plaques were observed 48 h post-infection. PFU values are calculated based on the average of at least 2 biological replicates and error bars represent the standard deviation \pm mean.

Table 1. Cytopathic effects (CPE) caused by EV-A71 mutants in comparison with the wild type EV-A71 strain 41.

EV-A71 Mutants	CPE
C475U	+
A486G	+++
G487A	+
VP1-98E	++
VP1-242K	+++
VP1-244K	+
G64R (3D ^{pol})	++
Partial Deletant (PD) 5'-NTR	+
VP1-E145G	+
VP2-149K	++++
2A-930K	++++
C272U	+++
T488C	+++
C700U	++
Multiple Mutant strain (MMS)	+
Positive Control (EV-A71 strain 41)	+++++

RD cells were infected with the EV-A71 wild type and mutant viruses at a MOI of 0.1. The TCID₅₀/ml values are calculated using the Reed and Muench formula determined from three independent experiments.

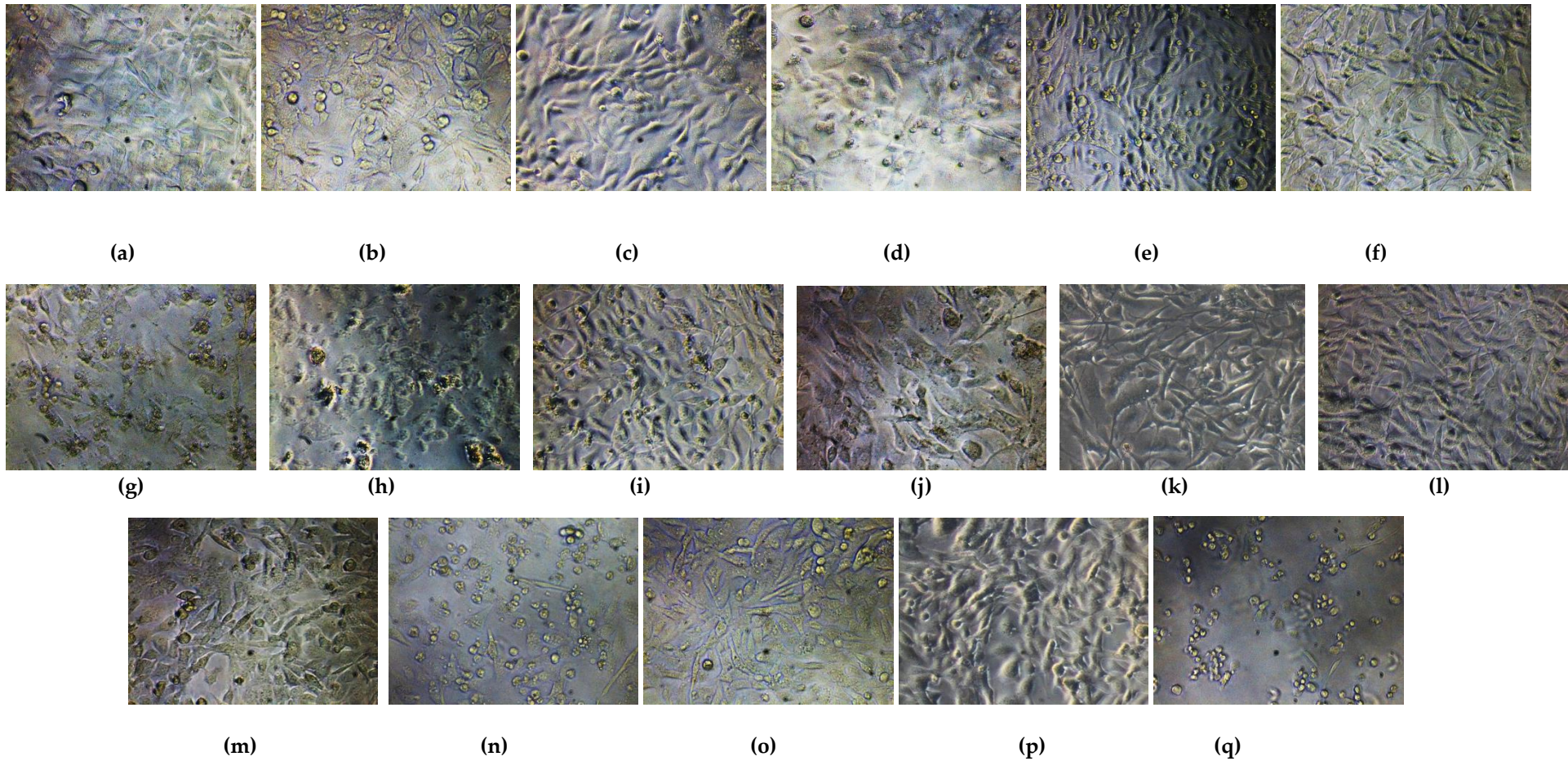


Figure 1. Cytopathic effects (CPE) caused by EV-A71 mutants (a) VP1-98E (b) VP1-242K (c) VP1-244K (d) G64R (e) PD (Partial Deletant 5'-NTR) (f) VP1-E145G (g) VP2-149K (h) 2A-930K (i) C272U (j) U488C (k) C700U (l) Multiple Mutant strain (MMS) (m) C475U (n) A486G (o) G487A in Rhabdomyosarcoma (RD) cells in comparison with (p) uninfected RD cells (negative control using Opti-MEM) and (q) EV-A71 wild type strain 41 infected RD cells (positive control).

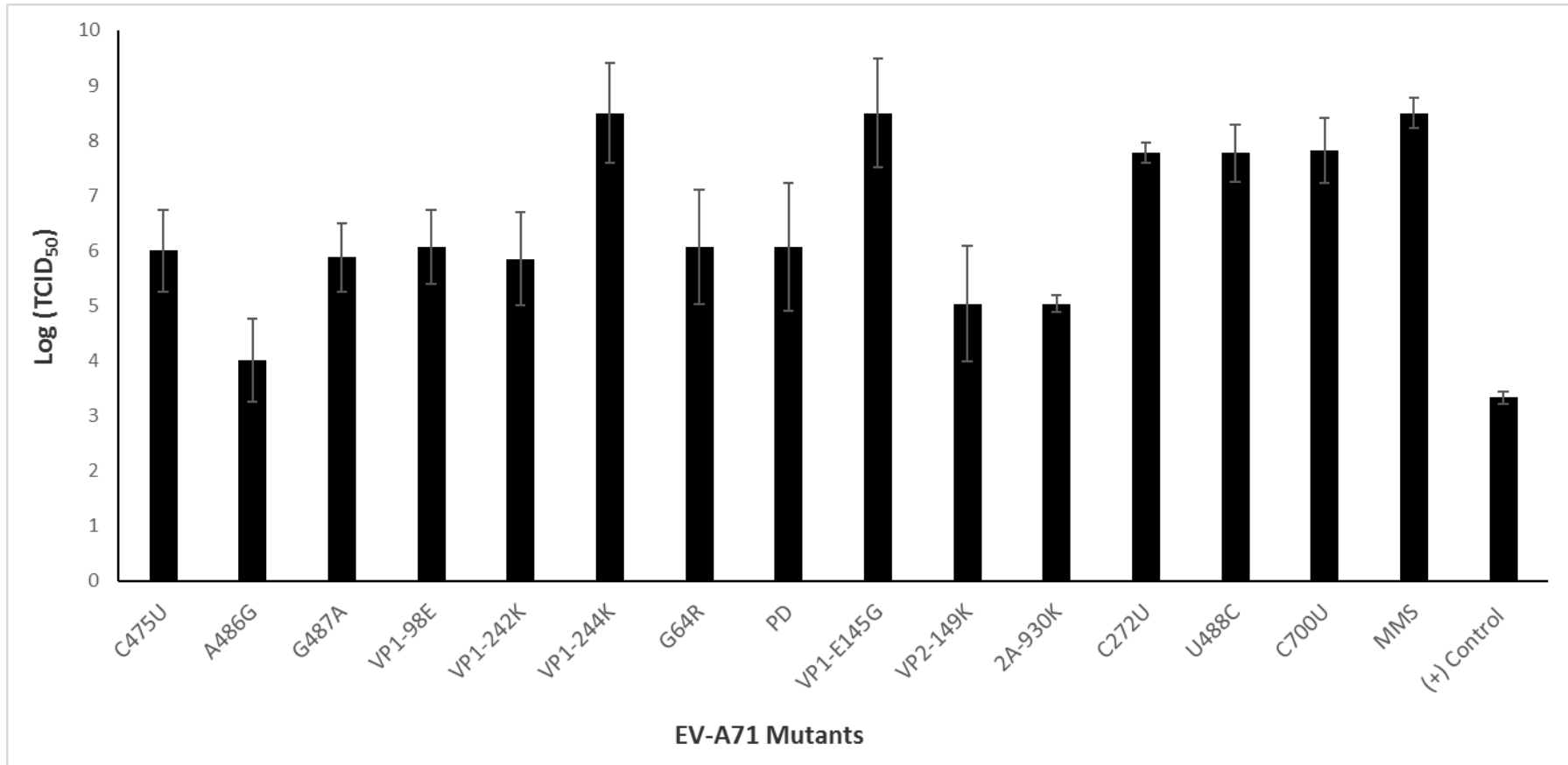


Figure 2. Logarithm Tissue Culture Infectious Dose 50 (Log TCID₅₀) of EV-A71 mutants in comparison with the wild type EV-A71 sub-genotype B4 strain 41. The plate was incubated at 37°C and observed daily for CPE up to 48h. The TCID₅₀/ml values are calculated using the Reed and Muench formula determined from at least three independent experiments.

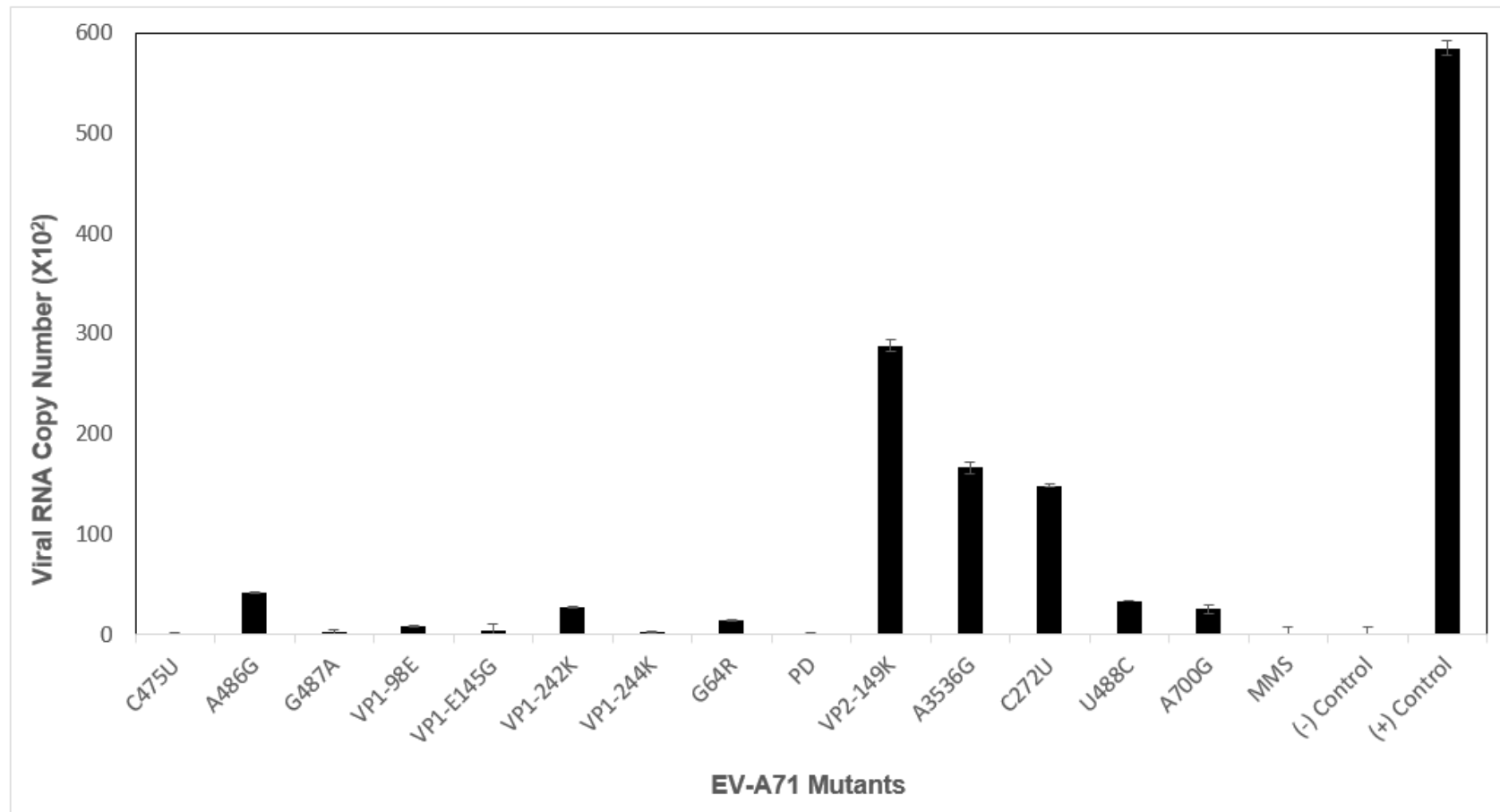


Figure 3. Quantification of Viral RNA Copy Number. Transfection of infectious RNA into RD cells was performed with the use of Lipofectamine 2000 reagent using EV-A71 mutants with a MOI of 0.1. (+) control refers to the EV-A71 sub-genotype B4 strain 41. (-) control refers to the RD cells with no virus infection. The viral RNA copy number was determined at 24h post-infection by TaqMan Real-Time PCR. Viral RNA copy numbers are the average of three biological replicates. Error bars represent the standard deviation of the mean.

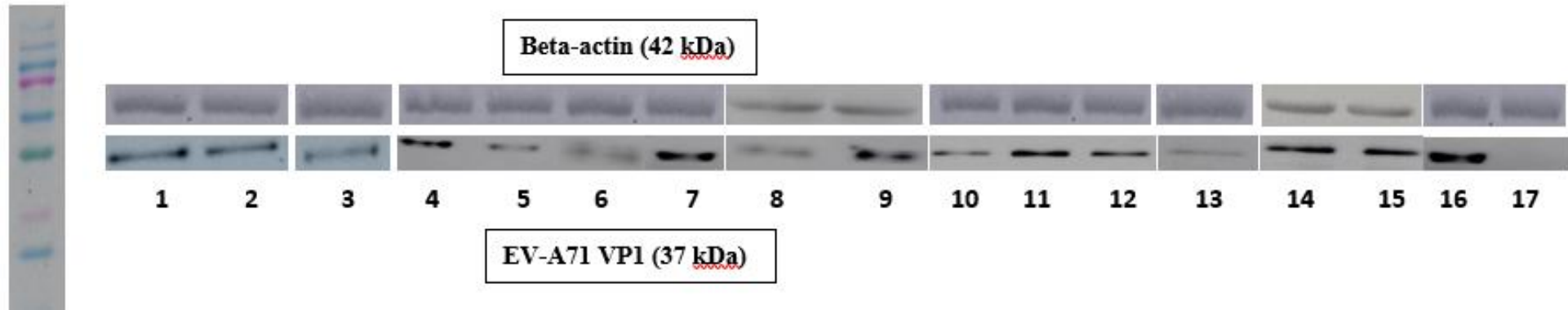
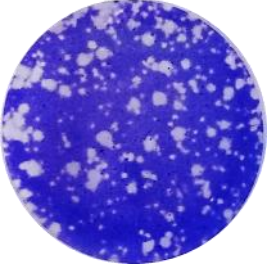
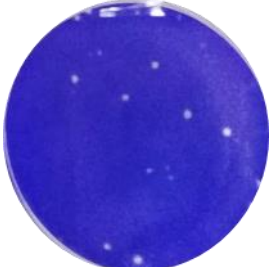
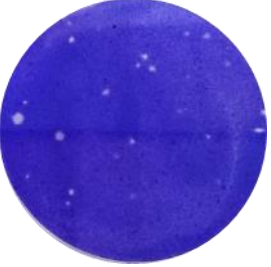

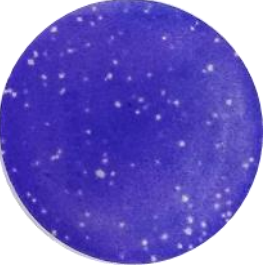
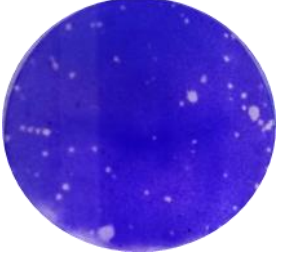
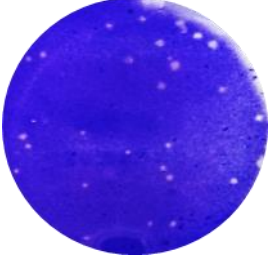
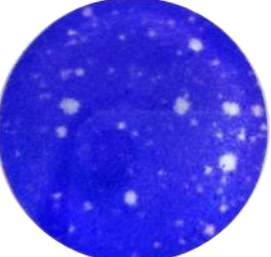


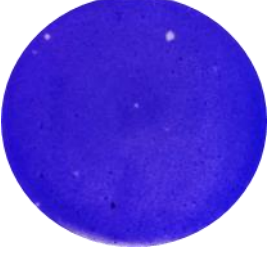
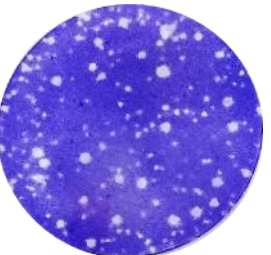
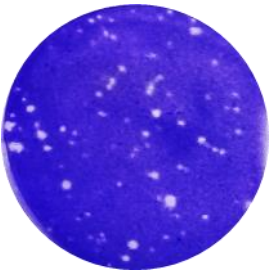

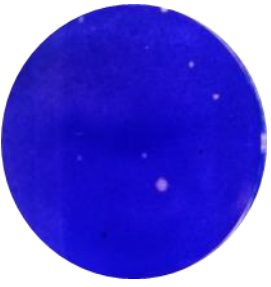


Figure 4. Western blot analysis using monoclonal antibody against VP1 as the primary antibody. The amount of EV-A71 total proteins and β -actin loaded in each lane was 20 μ g. The lanes are as follows: lane M, molecular weight marker (from 10 - 250 kilodaltons), lane 1, EV-A71 Mutant G64R; lane 2, Mutant VP1-98E; lane 3, Mutant VP1-E145G; lane 4, Mutant U488C; lane 5, Mutant G487A; lane 6, MMS; lane 7, A486G; lane 8, C475U; lane 9, Mutant VP1-242K; lane 10, Mutant VP1-244K; lane 11, Mutant C272U; lane 12, Mutant U700C; lane 13, Mutant Partial Deletant (PD); lane 14, VP2-149K; lane 15, 2A-930K; lane 16, Positive control (EV-A71 strain 41); lane 17, Negative control (uninfected RD cells). The molecular weights of the EV-A71 protein and β -actin are 36 kDa and 42 kDa, respectively.

<p>(a) Positive control</p>  <p>Viral count: 8.0×10^8</p>	<p>(b) VP1 (E145G)</p>  <p>Viral count: 3.5×10^5</p>	<p>(c) 3D (G64R)</p>  <p>Viral count: 6.0×10^6</p>	<p>(d) C475U</p>  <p>Viral count: 7.0×10^4</p>	<p>(e) A486G</p>  <p>Viral count: 2.3×10^7</p>
<p>(f) U488C</p>  <p>Viral count: 2.3×10^7</p>	<p>(g) VP1-242K</p>  <p>Viral count: 2.0×10^7</p>	<p>(h) C272U</p>  <p>Viral count: 5.7×10^7</p>	<p>(i) VP1-244K</p>  <p>Viral count: 2.5×10^5</p>	<p>(j) C700U</p>  <p>Viral count: 2.0×10^7</p>

<p>(j) Partial Deletant (PD)</p>  <p>Viral count: 1.0×10^5</p>	<p>(l) VP2-149K</p>  <p>Viral count: 9.9×10^7</p>	<p>(m) 2A-930K</p>  <p>Viral count: 7.0×10^7</p>	<p>(n) VP1-98E</p>  <p>Viral count: 7.5×10^5</p>	<p>(o) G487A</p>  <p>Viral count: 1.4×10^5</p>
<p>(p) MMS</p>	<p>(q) Negative control</p>			

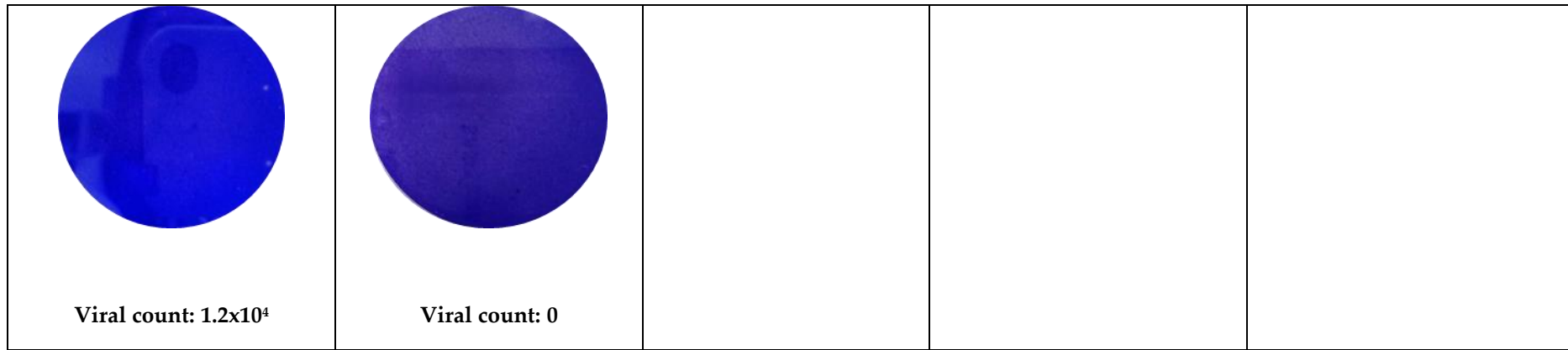


Figure 5. Quantification of plaque forming units by EV-A71 mutants and wild type EV-A71 strain 41. The plaque assays were performed on monolayer RD cells incubated at 37°C and were repeated at least two separate times.

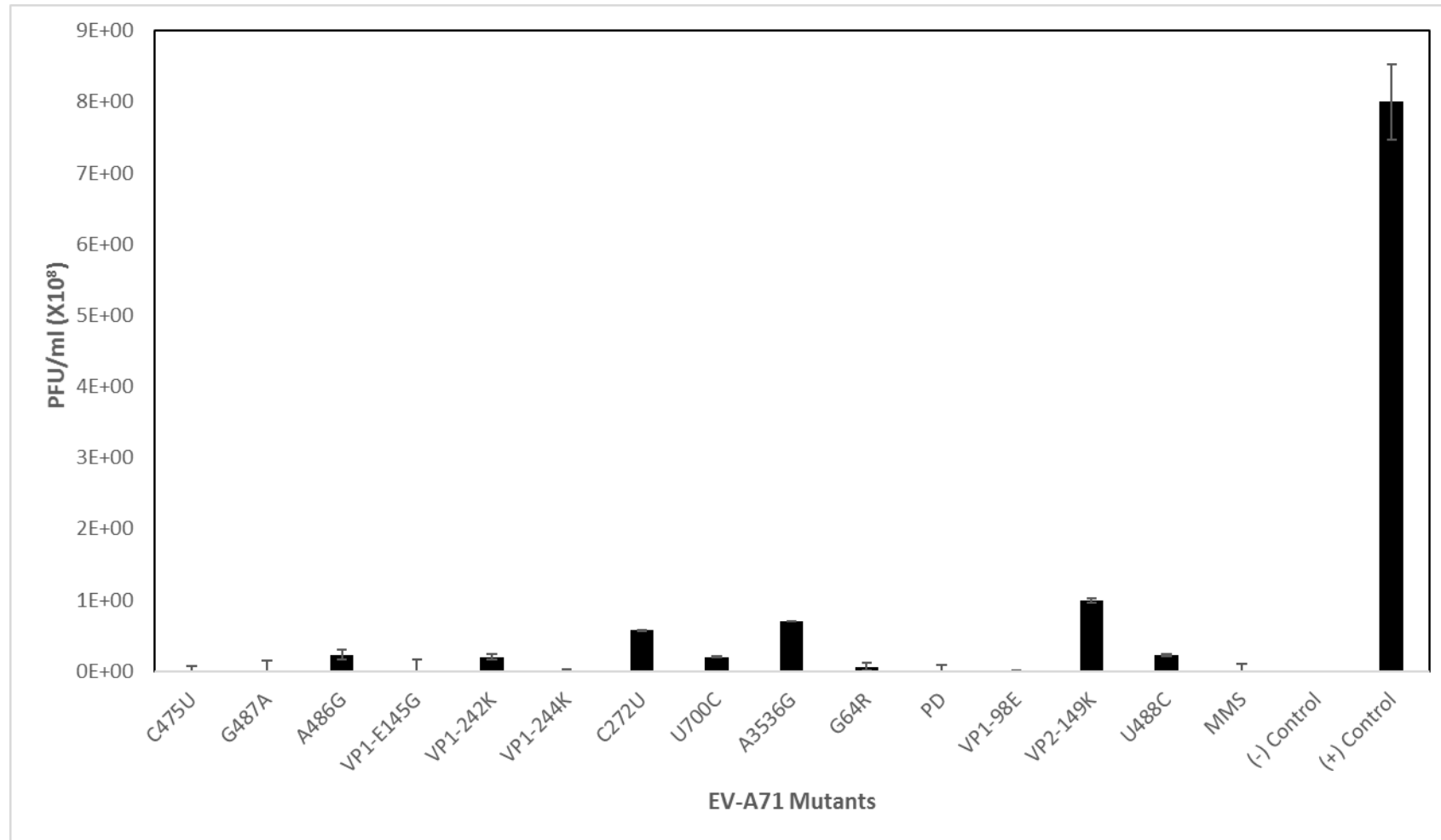


Figure 6. Plaque Forming Units by EV-A71 mutants and the wild type EV-A71 strain 41. RD cells were transfected with EV-A71 mutants and the wild type EV-A71 strain 41 at a MOI of 0.1. Plaque formation was observed 48 hours post-infection. PFU numbers are the average of two biological replicates; Error bars represent the standard deviation of the mean.